Journal of Archaeological Science 132 (2021) 105433

Contents lists available at ScienceDirect

Journal of Archaeological Science

journal homepage: www.elsevier.com/locate/jas

Deep learning reveals extent of Archaic Native American shell-ring building practices

Dylan S. Davis [a,**], Gino Caspari [b,c,*], Carl P. Lipo [d], Matthew C. Sanger [e]

[a] Department of Anthropology, The Pennsylvania State University, University Park, PA, 16802, USA
[b] Department of Archaeology, University of Sydney, Australia
[c] Institute of Archaeological Sciences, University of Bern, Switzerland
[d] Department of Anthropology, Binghamton University, Binghamton, NY, 13902, USA
[e] National Museum of the American Indian, Washington, D.C, 20560, USA

ARTICLE INFO

Keywords:
Settlement patterns
Deep learning
Shell rings
Object detection
Southeast United States

ABSTRACT

In the mid-Holocene (5000 - 3000 cal B.P.), Native American groups constructed shell rings, a type of circular midden, in coastal areas of the American Southeast. These deposits provide important insights into Native American socioeconomic organization but are also quite rare: only about 50 such rings have been documented to date. Recent work using automated LiDAR analysis demonstrates that many more shell rings likely exist than are currently recorded in state archaeological databases. Here, we use deep learning, a form of machine intelligence, to detect shell ring deposits and identify their geographic range in LiDAR data from South Carolina. We corroborate our results using synthetic aperture radar (SAR), multispectral data, and a random forest analysis. We conclude that a greater number of shell rings exist and that their distribution expanded further north than currently documented. Our evidence suggests that ring-construction was a more widespread and common practice during the mid-Holocene.

1. Introduction

Shell rings are circular middens composed of faunal and floral remains that contain a central plaza devoid of midden material (Russo, 2006; Sanger, 2017; Sanger and Ogden, 2018). These deposits are well-known in Southeastern archaeology (Fig. 1) and represent some of the first evidence for permanent human occupation in the coastal regions of the Atlantic and Gulf Coasts (Russo, 2006). The determination of past community structure that produced these shell-rings remains the subject of debate, with disagreements focusing on the degree to which deposits were a consequence of residence, ritual, or a mixture of activities (e.g., Russo, 2006; Sanger and Ogden, 2018; Thompson and Andrus, 2011; Trinkley, 1985).

Archaeologists have long posed questions about the patterns and scale of past community socio-cultural activities and their connections with neighboring regions (Kintigh et al., 2014). Within the Southeastern United States, scholarly understanding of the linkages between Native American communities that existed during the mid-Holocene (5000–3000 cal B.P.) are uncertain. While the archaeological record suggests that these ancient communities were closely interconnected (Bender, 1985; Sanger et al., 2018), the structure of relations among different locations remains unclear, particularly among communities associated with shell-ring architecture.

Despite being the subject of extensive investigations, our current knowledge of shell ring distributions is patchy, consisting of only ~50 such structures in the entirety of the American Southeast. Often located in poorly documented, dense coastal forests with limited access, these deposits are mostly known on the basis of large examples that are the most accessible to observation (Davis et al., 2020a). As a consequence, we lack a systematic inventory that would enable a comprehensive investigation into the range of environmental conditions in which rings are found, as well as good documentation of overall formal and compositional variability.

Documented shell rings are known to exist across an area ranging from Florida to South Carolina (Russo, 2006), though the actual geographic range of ring building practices is not definitively established. To date, the northernmost recorded shell ring deposit is the Sewee Shell Ring (38CH45). Located in Charleston County, SC, this

* Corresponding author. Department of Archaeology, University of Sydney, Australia.
** Corresponding author.
E-mail addresses: dsd40@psu.edu (D.S. Davis), gino.caspari@sydney.edu.au (G. Caspari).

https://doi.org/10.1016/j.jas.2021.105433
Received 8 March 2021; Received in revised form 28 May 2021; Accepted 22 June 2021
Available online 12 July 2021

circular ring dates to ca. 3675–4120 BP and has a diameter of 75 m and a height of 3.2 m (Russo, 2006). Given the insight provided by shell rings into sociopolitical organization, economic exchange networks, subsistence practices, and climate conditions (Anderson, 2004; Sanger et al., 2018; Trinkley, 1985), recording the extent of this cultural practice is of great importance for understanding changes in community organization throughout this region.

Here, we aim to systematically evaluate the geographic extent of shell ring building activities in the Archaic American Southeast. To achieve this, we use a Mask R-CNN deep learning model to remotely survey Beaufort, Charleston, and Georgetown Counties in SC for shell ring architecture (Fig. 1). We then corroborate these results using a random-forest (RF) probability analysis based on two additional sensors (synthetic aperture radar [SAR] and multispectral) and a manual evaluation of these results. Together these data offer a multi-pronged investigation into the archaeological record: LiDAR provides morphological information, SAR details soil properties, and multispectral highlights additional information about moisture content and vegetation. Thus, the integration of these datasets into an analysis offers new ways to investigate ring building cultures and improves our understanding of the likely spatial boundaries and commonality of shell ring building in the American Southeast.

2. Background

2.1. Shell ring architecture in the American southeast

The study of shell rings, middens, and other mounded structures has been a focal point of Southeastern archaeological research for over a century (Swallow, 1858; Claflin, 1931; Moore, 1894a; Putnam, 1875; Squier and Davis, 1848; Swallow, 1858). Extending from Mississippi and Florida to South Carolina, Archaic shell rings are found in primarily coastal settings and range in size from ~30 to 250 m in diameter and 1–6 m in height (Russo, 2006). The shape of these Archaic shell rings is likewise diverse, a property that scholars have suggested is reflective of sociopolitical organization (Anderson, 2004; Russo, 2004). Differences in ring size may also reflect differences in population density (Russo, 2006).

Data from investigations into the spatial and temporal patterns of mounded architecture have become foundational for establishing cultural chronologies, demography, environmental change, and social organization in past Native American societies (e.g., Moore , 1894b; Fairbanks, 1942; Ford and Willey, 1941; Moore, 1894a; Willey, 1939). Analyses of mound morphometry and distribution are often used as the basis for studies of demographic change, environmental alteration, social organization, and site formation in the Americas (e.g., Claassen, 1986; Crusoe and DePratter, 1976; Lightfoot and Cerrato, 1989; Peacock et al., 2005; Reitz, 1988; Russo, 2004; Trinkley, 1985).

Shell rings, a very specific form of midden, are quite rare. As such, knowledge of these features is still incomplete. There are many hypotheses surrounding shell rings, but many researchers account for rings as central points of residential and domestic activities of nucleated communities (Crusoe and DePratter, 1976; Thompson and Andrus, 2011; Trinkley, 1985). This is strengthened by recent evidence showing that shell ring locations were involved in both local-scale exchange with neighboring river valleys (Sanger, 2017), but also long-distance trade networks spanning hundreds of kilometers (Hill et al., 2019; Sanger et al., 2018).

Excavations of shell ring deposits largely support the notion that the areas in which they occur were occupied annually, given the year-round presence of the plant and animal species found at these locations (Calmes, 1967; Sanger et al., 2019; Thompson and Andrus, 2011;

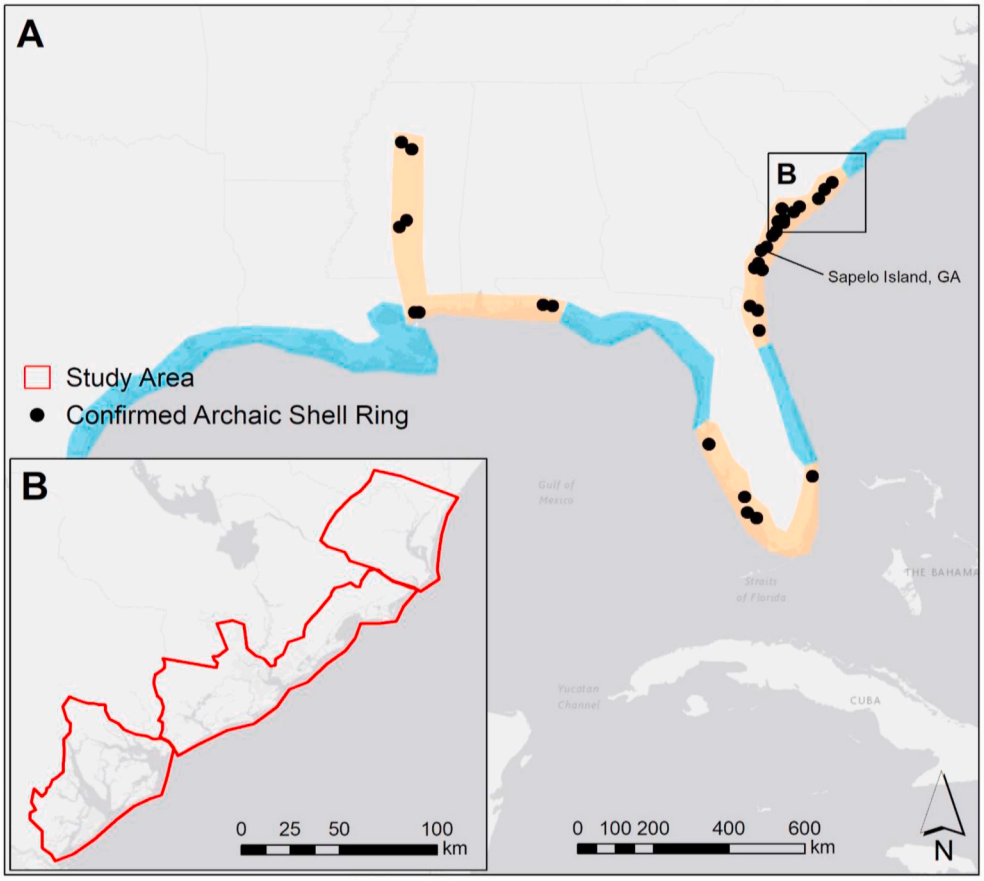

Fig. 1. Map of known shell ring locations. (A) Location of confirmed shell rings throughout the American Southeast (see Raymond, 2020; Russo, 2006). Highlighted areas show the known extent (orange) and potential extent (blue) of shell ring building activity. **(B)** The study areas (from south to north: Beaufort, Charleston, and Georgetown County). Service Layer Credits: ESRI, HERE, GARMIN, OpenStreetMap contributions, and the GIS User Community. (For interpretation of the references to colour in this figure legend, the reader is referred to the Web version of this article.)

Trinkley, 1985, 1980). In other cases, however, the deposits include shellfish that would have been harvested for only a fraction of the year, suggesting that occupation may have been seasonal (Sanger et al., 2019). Occupational patterns vary, however, as early residents may have been present year-round in some locations but later occupants were only present in certain seasons (Thompson and Andrus, 2011).

Some scholars reject the notion that these rings were living spaces. One hypothesis posits that shell rings were used as dam features to retain freshwater (Marquardt, 2010; Middaugh, 2013). According to this explanation, communities created shell rings during periods of low water availability, and these circular features captured water from rainfall, excavated wells, or stream overflow. Others believe that rings were occupations, but only for temporary episodic or ceremonial events (Sanger et al, 2018, 2019; Trinkley, 1985). The debate over the function of these ring features is important, as understanding how these structures were constructed and utilized provides insights into how Native Americans occupied the coastline of this region (Sanger et al., 2019).

While the distribution of documented shell rings does not extend further north than the Sewee Shell Ring in Charleston County, SC (Russo, 2006; Sanger et al., 2019; Saunders, 2017), recent research has documented a number of unrecorded shell ring features in this region using automated analyses of LiDAR data (Davis et al., 2019a, 2019b; also see Fig. 2). These deposits are considerably smaller than most currently known shell rings, which may explain their previous absence from archaeological records (Davis et al., 2020a). Given prior work, systematic evaluation of shell rings may reveal dozens of new shell rings that expand their geographic distribution further than previously thought (Davis et al., 2019b). This has important implications for our understanding of the Late Archaic social landscape in the American Southeast as it sheds light on the roles these structures served for members of these communities, which have been debated by scholars who primarily suggest that they may have served as ceremonial centers or common dwelling locations for coastal populations (Thompson and Turck, 2009).

2.2. Deep learning: Challenges and progress in archaeology

Deep learning, a branch of machine learning, has been rapidly gaining popularity among computational archaeologists in the past several years (Lambers et al., 2019; Caspari and Crespo, 2019; Trier et al., 2021, 2019; Verschoof-van der Vaart and Lambers, 2019). Convolutional Neural Networks (CNNs), in particular, have proven highly effective at increasing true positives while reducing false-positive results (Caspari and Crespo, 2019; Lambers et al., 2019; Somrak et al., 2020), which has been a longstanding problem in automated archaeological remote sensing analysis (Davis, 2019). Part of the reason for this improvement comes from how CNNs function: they take inputs from multidimensional matrices (known as tensors) which allow them to quantify multidirectional patterns, meaning that neighboring pixels influence the final identification (Caspari and Crespo, 2019). As such, CNNs are more sensitive to subtle patterns than other forms of machine learning.

Despite gains in popularity, applications of deep learning and other machine intelligence approaches within archaeology have been limited, partly due to a debate over their usefulness (Davis, 2020a), and also because of the amount of training data required, the computational power necessary to conduct these analyses, and the expertise required to develop these tools (Davis, 2020b). Shell rings are particularly rare features, and thus the compilation of hundreds or thousands of different examples to train a deep learning algorithm is not possible. Furthermore, morphological diversity among shell rings is high, as these features vary widely based on geographic location.

One solution to the need for large training datasets is transfer learning, wherein previously trained models can be used as a baseline for training a new model, in essence allowing for training data from

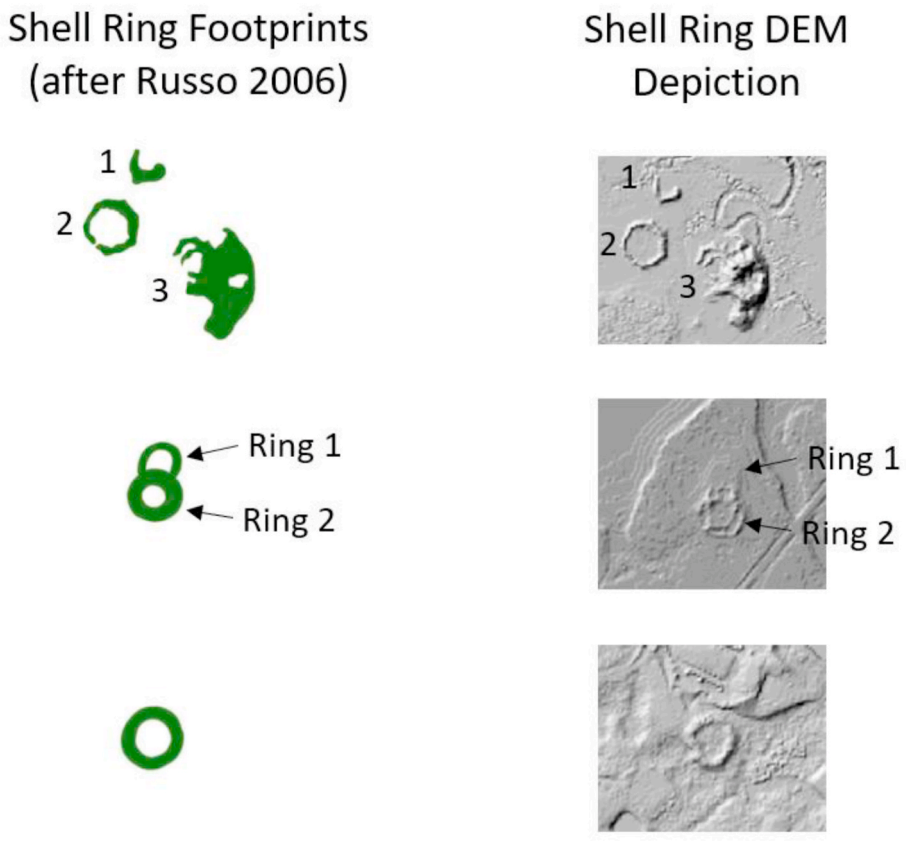

Fig. 2. Illustration of shell ring morphological footprints and how they appear in a LiDAR derived hillshade model. Notice that morphology is diverse, with some rings constituting full circles, others having multiple connected rings, and some which are more amorphous in shape.

previously implemented analyses to inform the creation of a new unrelated model (Tan et al., 2018). For archaeology, where training data is notoriously scarce, transfer learning techniques have provided a breakthrough in the automation of archaeological prospection research (Lambers et al., 2019).

With respect to the learning curve associated with deep learning, advances in GIS technology are now incorporating these complex methods. This can expand their utility among archaeologists and other scientists who may lack the high degree of expertise generally required to create and implement deep learning models. ArcGIS Pro (ESRI, 2020), for example, has a suite of tools for deep learning analyses of remote sensing datasets.

In this article, we demonstrate how shell rings can be detected using deep learning models trained with limited sample sizes by using augmentation (i.e., the creation of synthetic data to artificially increase training data sample sizes) and transfer learning techniques. Furthermore, we show how deep learning can be used to map geographic extents of human behavior which can contribute to broader theoretical discussions surrounding demographic shifts, sociopolitical domains, information exchange, and mobility.

3. Materials and methods

Our study makes use of a multipronged procedural workflow to detect shell rings, as depicted in Fig. 3. To start, we acquired LiDAR point data for Beaufort County (2390 km^2) and Georgetown County (805 km^2) from the National Oceanic and Atmospheric Administration (NOAA) with 1.3 m nominal point spacing and 15 cm vertical RMSE. We acquired LiDAR derived DEMs for Charleston County (3517 km^2) from the South Carolina Department of Natural Resources (DNR). These data have a 1.3 m nominal point spacing and 30 cm vertical RMSE. We created digital elevation models (DEMs) for Beaufort and Georgetown with 1.5 m spatial resolution by interpolating the LiDAR point data using inverse distance weighting (IDW). The Charleston LiDAR was downloaded as a DEM with 3 m spatial resolution. This raster was resampled to 1.5 m resolution using nearest-neighbor interpolation in ArcGIS Pro (ESRI, 2020) using the resample tool.

Next, we created two additional visualizations from LiDAR point data for each county: a hillshade map and a slope map. Both of these visualizations have improved object detection tasks within archaeology (Devereux et al., 2008). We then created a composite multiband raster in ArcGIS Pro consisting of these visualizations and the DEM. The deep learning framework in ArcGIS Pro requires multiband raster inputs.

3.1. MASK R–CNN models

Using this composite raster, we trained a Mask R–CNN architecture (He et al., 2017), which builds on Faster R–CNN models that have proven useful for detecting archaeological deposits (Lambers et al., 2019; Trier et al., 2021; Lambers et al., 2019), to locate archaeological mounds and shell rings from LiDAR derived raster data. Mask R–CNN models have only recently been used for archaeology (Bonhage et al., 2021; Dolejš et al., 2020).

Faster R–CNN uses a region proposal network (RPN), which is a small CNN that generates points in an image for the R–CNN model to look for objects (Ren et al., 2017). Regions of interest produced by the RPN are aligned in geographic space and run through two additional CNNs to create a mask of identified objects. These masks then segment detected objects which are classified by the Faster R–CNN.

Here, we design a Mask R–CNN model using ArcGIS Pro 2.6 to detect shell ring architecture using very limited training datasets and a ResNet 50 transfer learning backbone model. This model architecture can also be designed outside of ArcGIS Pro using Python (Python Software Foundation, 2020). We use Beaufort, Charleston, and Georgetown Counties in South Carolina as case studies. Beaufort County contains a large number of shell rings and represents an ideal location to acquire training data for rings located in South Carolina. Secondly, Beaufort was previously surveyed using automated remote sensing methods, revealing an abundance of new potential shell-ring sites (Davis et al, 2019b, 2020a). Charleston County is the location of the furthest northward extent of known shell ring deposits (Russo, 2006). Most of these rings are clustered towards southern and central Charleston County. As such, the area serves as a good location to test whether or not rings are found further north (i.e., Georgetown County) or whether the presently documented shell rings are the northern boundary of this cultural practice.

3.2. Implementing mask R–CNN in ArcGIS pro

Using the composite raster for the study region, we created training data using the Label Training Data for Deep Learning Analysis tool in ArcGIS Pro (ESRI, 2020). Beaufort County and Charleston County have large numbers of mound and ring features and we used these to generate training data for the Mask R–CNN model. We created training data consisting of 3 classes: shell rings, mounds, and modern (non-archaeological) objects. In total, we selected 18 shell rings (out of a total of 51 that are known in the entire Southeast), 21 circular mounds, and 36 modern structures (to alleviate false positives) as training samples.

Because of the limited knowledge of extant shell rings and mounds in this area, we needed to bolster our sample size using augmentation procedures. We augmented the training data using 45° rotations, thereby creating synthetic data that increased our sample sizes by a factor of 8. Using augmentation, we created a total of 776 images of shell rings, 720 mounds, and 1316 "modern" samples to check against false positives deriving from modern human activities. We then exported these training data as 200 × 200 pixel images with a stride size of 100 pixels using the Export Training Data for Deep Learning tool in ArcGIS Pro (Fig. 4a). Stride size is the number of pixels that the CNN filters at each level of analysis. Other image dimensions were tested (256 × 256, 150 × 150) but resulted in lower model performance.

Next we trained a Mask R–CNN model using a batch size of 6 and a ResNet50 backbone architecture (Fig. 4b). Batch size refers to the number of image tiles processed at one time. ResNet (Residual Network) 50 (He et al., 2017) is a transfer learning architecture that is trained on the ImageNet dataset (consisting of over 1 million images) with 50 layers and helps to improve both the speed and accuracy of the model training process. We set up the training procedure to run the model 50 times (50 epochs) and to stop training when the model was no longer improving, in order to save time and processing power. We trained the model on an unfrozen ResNet model because we did not have any previously trained models to work with for this area. Frozen models save time in model training and can be used in future work. To evaluate overfitting issues with the model, we withheld 10% of the training data for validation. We also test the model on data outside of our study region from Sapelo Island, Georgia, where 3 shell rings are located. These rings were not included in training data and serve as an additional check against overfitting from datasets beyond the confines of our study area in addition to the 10% of training data withheld when training the model.

Next, we evaluate the trained model's performance by detecting objects within the boundaries of Beaufort and Charleston County via the Detect Objects Using Deep Learning tool (Fig. 4c). Padding is used to limit detections made at the edge of a given analysis window, the threshold refers to the minimum confidence score that the model will treat as a positive detection, and the "return_boxes" parameter will draw boxes around a detected feature when True, which is the default. Following this analysis, we examined an 805 km^2 area from Georgetown County, directly north of Charleston County, to see if any additional ring features could be detected on the nearby coastal barrier islands.

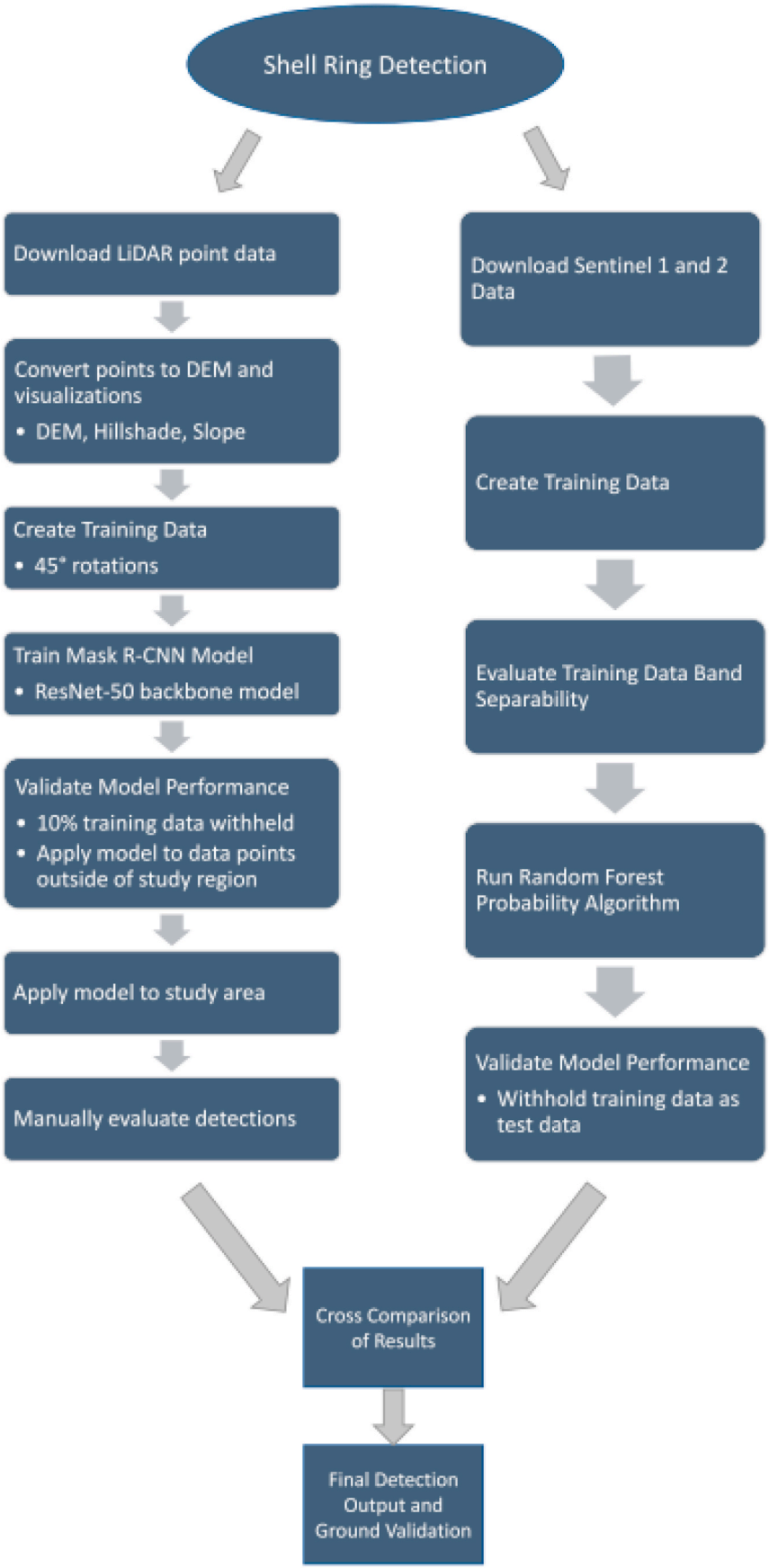

Fig. 3. Illustration of the methodological workflow implemented within this study.

Fig. 4. Settings used for constructing and implementing a Mask R–CNN model in ArcGIS Pro. **(A)** Export Training Data for Deep Learning Tool. **(B)** Train Deep Learning Model Tool. **(C)** Detect Objects Using Deep Learning Tool. The padding and threshold were lowered to 10 and 0.2, respectively, for Georgetown County to ensure maximum detection of potential rings.

3.3. Additional support of deep learning results

To provide verification of LiDAR derived deep learning results, we use multitemporal SAR data from Sentinel-1 and multispectral data from Sentinel-2 to conduct a random forest (RF) probability analysis of shell ring locations in the study region, following Orengo et al. (2020). Because this method works best in areas with limited vegetation cover, we use the analysis to evaluate the probability that detected shell rings in marshy areas without canopy cover are, in fact, archaeological. Sentinel 1 is a dual-polarization C-band SAR system with a spatial resolution of 10 m. SAR can reflect changes in topography, structure, surface roughness, and dielectric properties (i.e., soil moisture), all of which can indicate archaeological deposits (Chen et al., 2017; Comer and Blom, 2006; Lasaponara and Masini, 2013; Orengo et al., 2020). C-band SAR is particularly good at detecting structural changes and surface roughness associated with small archaeological sites composed of gravel, rocks, or in our case, shell (Comer and Blom, 2006). Sentinel-2 contains multispectral bands at 10 m resolution (and 20 m for SWIR) and can monitor distinct changes in vegetation, moisture retention, and soil composition.

Using a method published recently by Orengo et al. (2020), we create a multitemporal dataset consisting of 6 years of data totaling 510 Sentinel-1 SAR images using four bands consisting of single (HH and VV) and double (HHV and VVH) polarization sensors in ascending and descending order and 863 Sentinel-2 images using Google Earth Engine (GEE, (Gorelick et al., 2017)). Then we imported this data into R (R Core Team, 2020).

In R, we evaluated geophysical separability between confirmed shell rings and adjacent areas without shell rings in Sentinel-1 and Sentinel-2 data using a 10 m buffer. Because the Sentinel-1 data cannot penetrate dense vegetative canopies, we limit our analysis to shell rings located in marshes without heavy vegetation (n = 11) and select locations around these rings where no recorded archaeological materials are present (n = 33). Upon evaluation of band separability, we ran a RF probability algorithm in GEE using 9 of the confirmed shell rings as training data, while withholding 2 for validating the results. The RF model is trained using 128 trees and 3 iterations (following Orengo et al., 2020). RF models have been shown to perform well with a very limited amount of training information and are statistical classifiers that create decision trees using bootstrapping to classify a dataset (Breiman, 2001). We then re-evaluate the rings detected furthest north in our study area that are not covered in vegetation to provide an additional statistical metric of validation for these potential shell rings.

3.4. Ground validation

As a final assessment of our modeling results, we compared the detected shell ring and mound features from our Mask R–CNN and RF models to confirmed archaeological sites contained within the Department of Natural Resources (DNR) databases. We evaluate the overall performance of our automated detection efforts based on how many known shell ring deposits - including several intentionally excluded from model training - are correctly (re)identified. Because of the ongoing COVID-19 pandemic, it was not possible to conduct additional ground surveys at newly detected potential shell ring sites.

4. Results

Our Mask R–CNN model ran for 20 epochs with a learning rate of 6.30957e-06 before improvements stopped (Fig. 5). This required 41 h and 23 min to process on a computer with a NVIDIA Quadro p4000 GPU, an Intel® Core™ i7-7700 K CPU @ 4.20 GHz, 4200 Mhz, 4 Core(s), 8 Logical Processor(s), and 64 GB of RAM. The best model had a training and validation loss of 0.252 and 0.554, respectively (Fig. 5). Accuracy rated by validation data is reported in Table 1. Increases in training data will likely help rectify this issue in future research.

Using the training data to build the model, we were able to reidentify 17 out of 18 pre-documented shell rings (94.4%) and 17 out of 18 pre-documented mounds (94.4%). When applied to data beyond Beaufort and Charleston Counties, the model detected 1 out of 3 rings located in

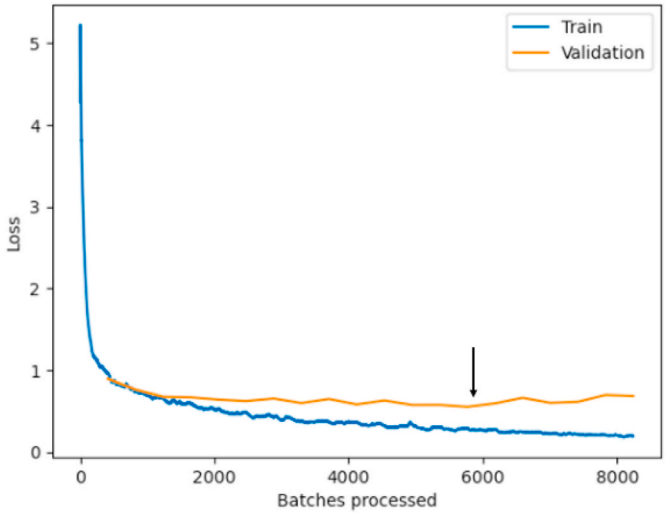

Fig. 5. Mask R–CNN model performance. The two curves loss values associated with model training. The lower the loss, the more reliable the model. The black arrow indicates the best performing model, which attained the lowest loss values during training.

Table 1
Accuracy metrics of Mask R–CNN model: Data accuracy ratings for shell rings, mounds, and modern features (used to reduce false positive detections) based on the 10% training sample withheld for validation. ArcGIS Pro provided accuracy rather than sensitivity or precision scores, which can be found in the supplemental files.

Feature class	Validation accuracy
Shell ring	75%
Mound	79.5%
Modern	59.5%

Sapelo Island, with the two undetected rings consisting of destroyed features (Fig. 6; see Russo, 2006). Thus, the model successfully identifies well-preserved shell rings but needs further improvements to successfully locate damaged deposits.

We applied this trained model to the Beaufort and Charleston County data and identified a total of 2035 rings and 3254 mounds. Next, we manually evaluated the results to reduce false positives related to modern development and natural topographic and hydrological features. We noted that many identifications were false positives related to natural hydrological phenomena (e.g., river channels) and some were the result of modern development activity. As such, we paid attention to the immediate surroundings of each detected object and removed all those which were located in urban environments, developed land, or were the result of natural topographic phenomena (like riverbanks). After manual evaluation, the total number of identified rings was 120 (52 in Beaufort and 91 in Charleston) and mounds totaled 287 (87 in Beaufort and 200 in Charleston) (Fig. 7). Several of these rings are located further north than Sewee Shell Ring (38CH45), the northernmost shell ring identified to date.

When we applied the model to Georgetown County, we lowered the confidence threshold to 0.2 to ensure that we did not miss potential rings. In prior tests we used higher thresholds but found that morphological differences between training data and new rings lowered their chances of detection. As such, we used a lower threshold. With this configuration, the model identified only 63 objects as shell rings, far fewer than Charleston or Beaufort County. Upon manual evaluation of these potential rings, 5 are likely to be archaeological rings due to their

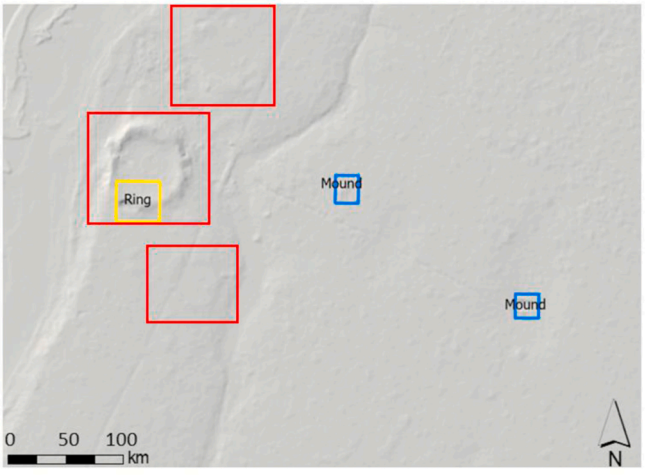

Fig. 6. The Sapelo Island Shell Ring Complex. The yellow rectangle shows the area identified as a ring by the Mask R–CNN model (and Sapelo Ring 1). The three red boxes indicate the boundaries of the three rings in this area, two of which were not detected by the model. Both rings that were not detected are listed as destroyed by Russo (2006) and display only faint topographic traces in the DEM. (For interpretation of the references to colour in this figure legend, the reader is referred to the Web version of this article.)

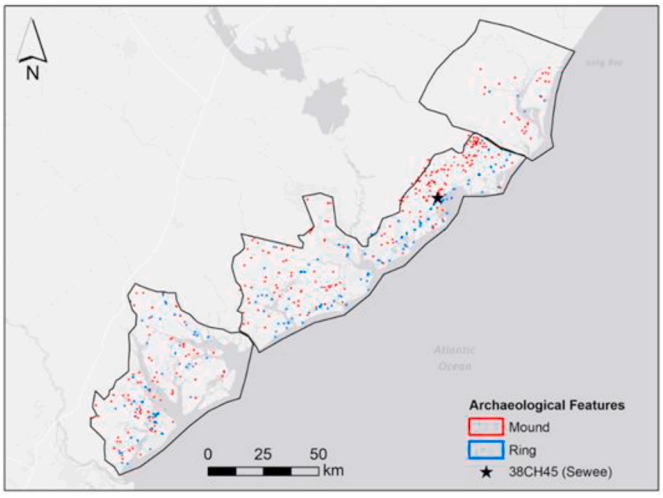

Fig. 7. Results of Mask R–CNN analysis. Locations of identified shell ring and mound features throughout the study region.

environmental context and morphological characteristics. The northernmost ring that we were able to detect is 53 km further north than the Sewee shell ring (38CH45). Additionally, the model detected 93 potential mound deposits, 25 of which appear to be artificial and pre-European contact in age.

4.1. Additional assessment of shell rings using SAR, multispectral, and random forest probability

Minimizing false positives requires the evaluation of independent data. To verify the Mask R–CNN results, we used SAR and multispectral data to train a random forest (RF) classifier to identify shell rings. Initial assessments of SAR and multispectral bands showed clear differences between shell rings and non-archaeological areas (Figs. S1 and S2). Results of SAR analysis show distinct differences between confirmed and suspected archaeological shell rings and the surrounding landscape (Fig. 8; Fig. S3). Shell rings display lower average reflectance values in both the single and double polarization bands, but the differentiation is clearer in single-polarization bands (Fig. 8). This pattern indicates that archaeological sites are relatively smooth compared to the surrounding marshland and likely trap high-degrees of moisture due to clumped organic materials, leading to less energy being reflected back to the sensor (Comer and Blom, 2006; Elfadaly et al., 2020).

The detected shell rings display closer similarities with confirmed shell rings than non-archaeological features. In the single polarization Sentinel-1 SAR bands (VV Ascending, VV Descending), confirmed and detected shell rings are statistically different from non-archaeological features (p-value < 0.04) and similar to each other (p-value > 0.6), while in dual-polarization bands (VV + VH Ascending and VV + VH Descending) all features are statistically similar to each other (p-value > 0.1).

Multispectral analysis from Sentinel-2 also shows distinct differences between confirmed and suspected shell rings and surrounding areas, but the potential shell rings also appear distinct from the sample of confirmed shell rings (Fig. 9). These results indicate that shell rings display higher moisture retention properties, distinct soil signatures, and distinct vegetation patterns compared to surrounding areas. The difference between confirmed and suspected shell rings may be the result of low-spatial resolution (10–20 m), diversity among shell ring signatures, or the possibility that some of the detected shell rings are not archaeological. Given the statistical difference between known non-archaeological locations and the suspected shell rings, followed by the results of the RF-probability analysis (discussed below), we believe that the first two explanations are the most probable.

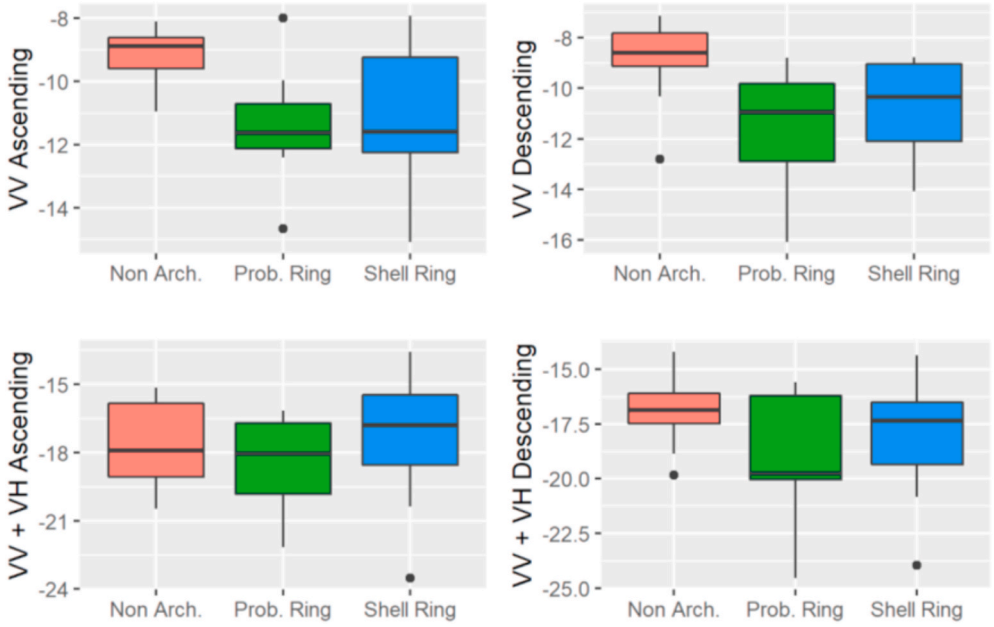

Fig. 8. Results of SAR band evaluation. Comparison of C-band SAR reflectance values between non-archaeological areas surrounding shell rings (n = 33), detected shell rings (n = 12), and confirmed shell rings (n = 11). Non Arch. refers to non-archaeological areas. Prob. Ring refers to probable rings detected by the Mask R–CNN model.

Fig. 9. Results of Sentinel-2 band evaluation. Comparison of Sentinel-2 band reflectance values between non-archaeological areas (n = 33), detected shell rings (n = 12), and confirmed shell rings (n = 11). Non Arch. refers to randomly generated ground points outside of known shell rings without any archaeological remnants, Prob. Ring refers to probable rings detected by the Mask R–CNN model.

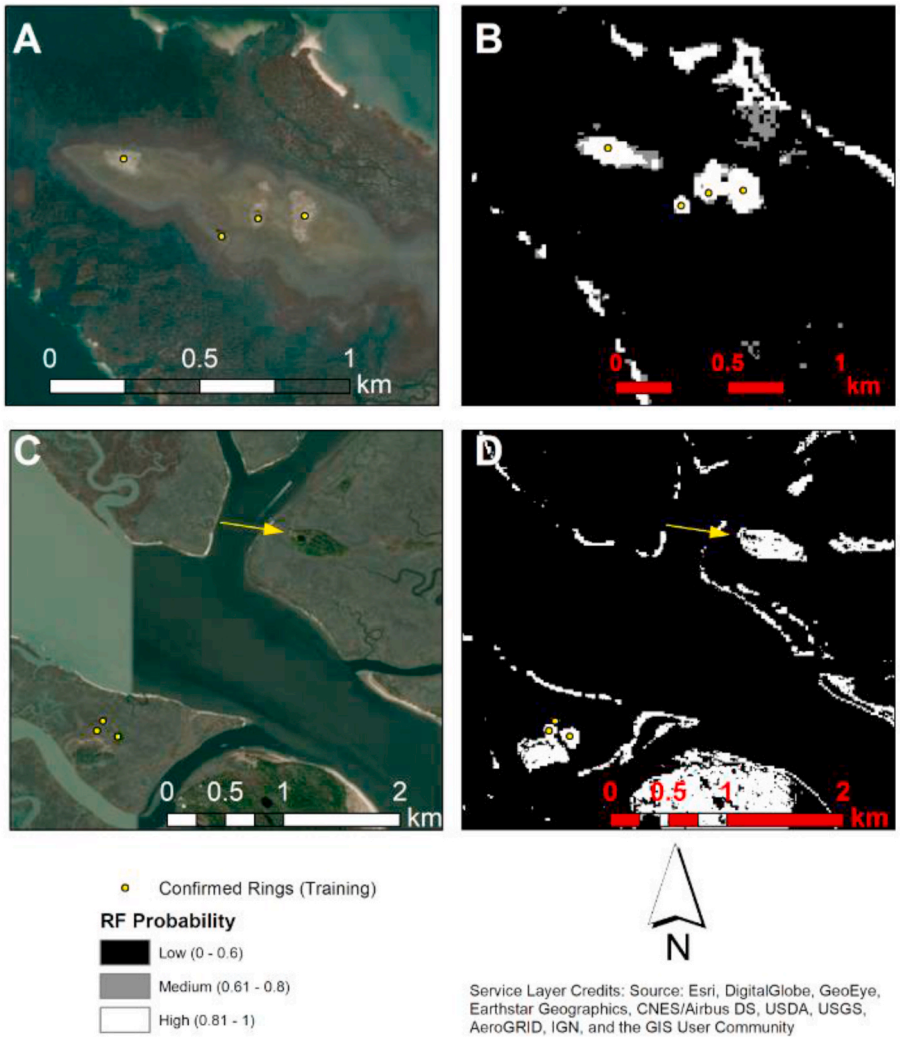

Fig. 10. Results of Random Forest probability classifier. White areas represent locations that are identified as shell rings at a probability of ≥0.5. Yellow dots represent confirmed rings used as training data. Yellow arrows represent confirmed rings withheld as validation data. (For interpretation of the references to colour in this figure legend, the reader is referred to the Web version of this article.)

We conducted an RF-probability analysis using a multitemporal and multisensor approach (Fig. 10). We noted band separability between confirmed shell rings and surrounding environmental contexts (Figs. 8 and 9). Our RF analysis re-identifies all 9 confirmed rings used as training data and an additional 2 rings withheld as validation. RF also identifies 9 of the 12 potential shell rings detected by the deep learning model north of Sewee Shell Ring using a threshold of 0.5. Further evaluation of these potential shell rings shows that their spectral characteristics are also statistically different ($p < 0.05$) from areas without shell rings.

4.2. Ground validation

According to the DNR, a total of 47 identified ring and mound features are located within DNR lands. These 47 features consist of 22 confirmed archaeological deposits, many of which were not used as training data for the DL or RF models. This list includes a known Archaic era shell ring, Archaic and Mississippian era mounds, and two historic features (Table 2). In total, there were 4 shell rings located on DNR lands that we did not include in our training dataset, of which our model identified half. Thus, while not perfect, our automated analyses performed well enough to locate additional archaeological features beyond known training examples, including shell ring sites from the Archaic period.

Table 2
Confirmed archaeological sites identified by Mask R–CNN model. Selection of recorded archaeological sites within DNR jurisdiction identified using the designed deep learning model.

Site ID	Site type	Used as training data (Y/N)
38BU0303	Archaic shell ring	N
38BU0304	Archaic shell ring	Y
38BU0300	Archaic shell ring	Y
38BU0348	Woodland era mound	N
38CH0042	Archaic shell ring	Y
38CH0556	Shell bearing site (possible ring)	N
38CH1213	Historic mound	N
38GE0450	Historic mound	N
38GE0449	Historic mound	N

5. Discussion

Prior to this investigation, no shell rings were documented north of Charleston County, South Carolina. Previous investigations of shell rings, however, were largely opportunistic surveys, resulting in a patchy understanding of their total geographic distribution (Davis et al.,

2020a). Using deep learning and LiDAR data, we illustrate that ring building was more widespread than previously thought (also see Davis et al., 2019a, 2019b). We scanned a total of 6712 km^2 in South Carolina using deep learning and identified 120 potential shell rings within Beaufort and Charleston Counties. Our results are consistent with prior semi-automated attempts to quantify shell rings in this area (Davis et al., 2019a, 2019b) but also add an additional 5 shell rings in Georgetown County to the known inventory.

Relatively speaking, density of identified rings decreased substantially as we moved further north, justifying the notion that shell ring building does not extend much beyond South Carolina. We validated these conclusions by analyzing these potential rings using an RF classifier based on SAR and multispectral data. This analysis also suggests that these deposits are artificial in origin and pre-European contact in age. Thus, using three different sensors, two different automation methods, and manual evaluation, we were able to validate the shell rings detected in this study. Significantly, the shell rings identified in Georgetown are the northernmost known examples of shell ring building ever recorded in North America. This finding has important implications for our understanding of Archaic fishing communities and their variability throughout the coastal Southeast.

With the discovery of dozens of new shell rings, the status of these features shifts from being rare cases of monumental architecture to a relatively common practice that was shared by a wide array of coastal-dwelling communities across a substantial portion of Southeastern North America. While the results of our deep learning model may have missed some potential rings in the Georgetown area, as validation only achieved 75% accuracy, it is possible that additional shell rings exist within this region. With increases in training data, the performance of the model developed here can be improved to detect a greater proportion of extant shell rings in the American Southeast. Nonetheless, our results provide two major insights into the settlement history of this region: 1) the geographic range of shell-building practices extends further north than previously recorded; and 2) while some shell rings may have acted as rare monuments, a more likely function was as common domestic structures.

The rings detected in Georgetown County by our deep learning model (confidence ratings of 0.98, 0.97, 0.85, 0.54 and 0.54 and also identified with an RF algorithm) suggests that the geographic range of shell ring building expands over 50 km further to the north. Each of these rings is located near barrier islands and within 10 km of each other. This pattern follows examples of other documented shell rings along the Georgia and South Carolina Coasts that are often located within 20–30 km of the next closest ring. Given that the data we analyzed only extends 10 km further north of the rings identified in Georgetown, it is likely that other rings may exist beyond the boundaries of this current study. Barrier islands, however, become scarcer the further one travels north towards North Carolina. Thus, it is also possible that shell ring building subsides as barrier islands become less common in coastal environments. We also note that the total number of detected ring features was significantly lower for Georgetown County than any of the other areas of our study region, despite using a lower detection threshold, reflecting what is likely a decrease in the overall numbers of these features as one moves northward.

The documentation of ring-building activities also provides potential opportunities to study mobility patterns and subsistence strategies of Archaic period Native Americans which have historically been limited by small sample sizes of available material present in these middens (Sanger et al., 2019). Recent work on shell rings shows how these deposits can provide key information pertaining to marine resource exploitation patterns, and therefore provide key insights to dealing with resource sustainability (Cannarozzi and Kowalewski, 2019). The identification of new potential shell rings opens the possibility for broader comparative analyses of resource exploitation patterns throughout the American Southeast which may hold implications for sustainable shell-fishing in the present.

Newly discovered shell rings are already contributing new information. For example, Davis et al. (2020a) demonstrate that shell ring distribution is influenced by elevation levels and the presence of other shell ring sites, suggesting that these rings served a central function in social connectivity between communities. Furthermore, many rings discovered in LiDAR data (Davis et al., 2019a, 2019b) are smaller than previously documented deposits. This pattern holds in this study, as the average area of identified shell rings (4331.62 m^2) is substantially smaller than pre-documented rings (5980.77 m^2) within the study region. The spatial patterns of pre-documented rings suggest a highly integrated socio-economic structure between communities living at and around shell rings (Davis et al., 2020a; Sanger, 2017; Sanger et al., 2018).

With continued research, the shell rings identified here can be explored to generate information about their age. Such investigations will then offer new additions to our training data. Additions to training data will assist in the development of new deep learning models that improve upon the accuracy of detections and that have broader applicability. Such methods can play a major role in identifying shell ring sites in areas where there are currently gaps in our knowledge. For example, in Florida, there are large swaths of coastline for which there currently appear to be no shell rings (Fig. 1) given the density of shell rings further north in Georgia and South Carolina, however, these stretches of land may contain dozens of unrecorded shell rings. Ground-verification of potential shell rings identified here (particularly in Georgetown County) will offer a significant contribution to our understanding of the geographic extent of shell-building practices and their role within Archaic Native American societies.

6. Conclusion

Archaeological sites in the American Southeast are at risk of disappearing due to climate change and development activities (Anderson et al., 2017; Davis et al., 2020b). As such, we must find ways to expedite our data processing capabilities to ensure adequate protection and study of at-risk cultural heritage (Soroush and Khazraee, 2020). As we demonstrate here, deep learning and automation can be used to not only detect new archaeological features, but also to systematically estimate the spatial extents of certain archaeological building traditions. Using multiple data sources (i.e., LiDAR, SAR, multispectral) and new analytic methods, we have systematically detected over 100 extant shell rings throughout South Carolina, alone. We further quantify the geographic range of this building tradition and demonstrate that many of these features are quite small compared to known examples, which suggests that not all shell rings were used as monumental ceremonial centers. This approach helps not only in documenting cultural deposits, but also in explaining the archaeological record, which remains limited in many automated remote sensing studies (Davis, 2019).

As work continues, information from these newly documented shell rings may help to clarify the role that ring building had in Archaic Native American communities, as well as the range of socioeconomic networks between coastal dwelling groups in this area. The deep learning model and all code used for analysis is freely available (see supplemental files) and we hope that future researchers can use this work to improve upon our results.

Data availability

The deep learning model and training data created in this study are available through Penn State's ScholarSphere repository at https://doi.org/10.26207/ry6k-q463. Code for R and GEE analyses is provided in the supplemental document. Training data are provided in two formats: Pascal-VOC objects (a standard deep learning format) and Mask-RCNN format (which is used in ArcGIS Pro for training Mask-RCNN models). The trained Mask-RCNN model is provided as an ArcGIS Pro Deep Learning Package (.dlpk), and can be used by anyone with an ArcGIS Pro

license.

Declaration of interest statement

The authors declare that they have no conflicts of interest with regards to this manuscript or its contents.

Acknowledgements

We thank Karen Smith and Meg Gaillard for sharing DNR archaeological records with us. We also extend our appreciation to the two anonymous reviewers who provided valuable feedback on a previous version of this article. G. Caspari was funded by the Swiss National Science Foundation, grant number P400PG_190982.

Appendix A. Supplementary data

Supplementary data to this article can be found online at https://doi.org/10.1016/j.jas.2021.105433.

Funding

No specific funding was provided for this study.

References

Anderson, D.G., 2004. Archaic mounds and the archaeology of southeastern tribal societies. In: Gibson, J.L., Carr, P.J. (Eds.), Signs of Power: the Rise of Cultural Complexity in the Southeast. University of Alabama Press, Tuscaloosa, pp. 270–299.

Anderson, D.G., Bissett, T.G., Yerka, S.J., Wells, J.J., Kansa, E.C., Kansa, S.W., Myers, K. N., DeMuth, R.C., White, D.A., 2017. Sea-level rise and archaeological site destruction: an example from the southeastern United States using DINAA (Digital Index of North American Archaeology). PloS One 12, e0188142. https://doi.org/10.1371/journal.pone.0188142.

Bender, B., 1985. Emergent tribal formations in the American midcontinent. Am. Antiq. 52–62.

Bonhage, A., Eltaher, M., Raab, T., Breuß, M., Raab, A., Schneider, A., 2021. A modified Mask region-based convolutional neural network approach for the automated detection of archaeological sites on high-resolution light detection and ranging-derived digital elevation models in the North German Lowland. Near E. Archaeol. https://doi.org/10.1002/arp.1806. Prospect. n/a.

Breiman, L., 2001. Random forests. Mach. Learn. 45, 5–32.

Calmes, A.R., 1967. Test excavations at two late archaic sites on hilton head island. In: Presented at the Southeastern Archaeological Conference, Macon, GA.

Cannarozzi, N.R., Kowalewski, M., 2019. Seasonal oyster harvesting recorded in a Late Archaic period shell ring. PloS One 14, e0224666. https://doi.org/10.1371/journal.pone.0224666.

Caspari, G., Crespo, P., 2019. Convolutional neural networks for archaeological site detection – finding "princely" tombs. J. Archaeol. Sci. 110, 104998. https://doi.org/10.1016/j.jas.2019.104998.

Chen, F., Lasaponara, R., Masini, N., 2017. An overview of satellite synthetic aperture radar remote sensing in archaeology: from site detection to monitoring. J. Cult. Herit. 23, 5–11. https://doi.org/10.1016/j.culher.2015.05.003.

Claassen, C., 1986. Shellfishing seasons in the prehistoric southeastern United States. Am. Antiq. 51, 21–37.

Claflin, W.H., 1931. The Stalling's Island Mound, Columbia County, Georgia, Papers of the Peabody Museum of American Archaeology and Ethnology. Harvard University, Cambridge. Papers of the Peabody Museum of American Archaeology and Ethnology, Harvard University.

Comer, D.C., Blom, R.G., 2006. Detection and identification of archaeological sites and features using synthetic aperture radar (SAR) data collected from airborne platforms. Remote Sensing in Archaeology. Springer, pp. 103–136.

Crusoe, D.L., DePratter, C.B., 1976. New look at the Georgia coastal shell mound archaic. Fla. Anthropol. 29, 1–23.

Davis, D.S., 2020a. Defining what we study: the contribution of machine automation in archaeological research. Digit. Appl. Archaeol. Cult. Herit. 18, e00152 https://doi.org/10.1016/j.daach.2020.e00152.

Davis, D.S., 2020b. Geographic disparity in machine intelligence approaches for archaeological remote sensing research. Rem. Sens. 12, 921. https://doi.org/10.3390/rs12060921.

Davis, D.S., 2019. Object-based image analysis: a review of developments and future directions of automated feature detection in landscape archaeology. Archaeol. Prospect. 26, 155–163. https://doi.org/10.1002/arp.1730.

Davis, D.S., DiNapoli, R.J., Sanger, M.C., Lipo, C.P., 2020a. The integration of lidar and legacy datasets provides improved explanations for the spatial patterning of shell rings in the American Southeast. Adv. Archaeol. Pract. 8, 361–375. https://doi.org/10.1017/aap.2020.18.

Davis, D.S., Lipo, C.P., Sanger, M.C., 2019a. A comparison of automated object extraction methods for mound and shell-ring identification in coastal South Carolina. J. Archaeol. Sci. Rep. 23, 166–177. https://doi.org/10.1016/j.jasrep.2018.10.035.

Davis, D.S., Sanger, M.C., Lipo, C.P., 2019b. Automated mound detection using lidar and object-based image analysis in Beaufort County, South Carolina. SE. Archaeol. 38, 23–37. https://doi.org/10.1080/0734578X.2018.1482186.

Davis, D.S., Seeber, K.E., Sanger, M.C., 2020b. Addressing the problem of disappearing cultural landscapes in archaeological research using multi-scalar survey. J. Isl. Coast. Archaeol. https://doi.org/10.1080/15564894.2020.1803457 (in press).

Devereux, B.J., Amable, G.S., Crow, P., 2008. Visualisation of LiDAR terrain models for archaeological feature detection. Antiquity 82, 470–479. https://doi.org/10.1017/S0003598X00096952.

Dolejš, M., Pacina, J., Veselý, M., Brétt, D., 2020. Aerial bombing crater identification: exploitation of precise digital terrain models. ISPRS Int. J. Geo-Inf. 9, 713. https://doi.org/10.3390/ijgi9120713.

Elfadaly, A., Abate, N., Masini, N., Lasaponara, R., 2020. SAR Sentinel 1 imaging and detection of palaeo-landscape features in the mediterranean area. Rem. Sens. 12, 2611. https://doi.org/10.3390/rs12162611.

ESRI, 2020. ArcGIS Pro. Environmental Systems Research Institute, Inc., Redlands, CA.

Fairbanks, C.H., 1942. The taxonomic position of stalling's island, Georgia. Am. Antiq. 7, 223–231.

Ford, J.A., Willey, G.R., 1941. An interpretation of the prehistory of the eastern United States. Am. Anthropol. 43, 325–363.

Gorelick, N., Hancher, M., Dixon, M., Ilyushchenko, S., Thau, D., Moore, R., 2017. Google Earth engine: planetary-scale geospatial analysis for everyone. Remote Sens. Environ. 202, 18–27.

He, K., Gkioxari, G., Dollár, P., Girshick, R., 2017. Mask r-cnn. Proceedings of the IEEE International Conference on Computer Vision, pp. 2961–2969.

Hill, M.A., Lattanzi, G.D., Sanger, M., Dussubieux, L., 2019. Elemental analysis of late archaic copper from the McQueen Shell ring, St. Catherine's island, Georgia. J. Archaeol. Sci. Rep. 24, 1083–1094.

Kintigh, K.W., Altschul, J.H., Beaudry, M.C., Drennan, R.D., Kinzig, A.P., Kohler, T.A., Limp, W.F., Maschner, H.D.G., Michener, W.K., Pauketat, T.R., Peregrine, P., Sabloff, J.A., Wilkinson, T.J., Wright, H.T., Zeder, M.A., 2014. Grand challenges for archaeology. Am. Antiq. 79, 5–24. https://doi.org/10.7183/0002-7316.79.1.5.

Lambers, K., Verschoof-van der Vaart, W., Bourgeois, Q., 2019. Integrating remote sensing, machine learning, and citizen science in Dutch archaeological prospection. Rem. Sens. 11, 794. https://doi.org/10.3390/rs11070794.

Lasaponara, R., Masini, N., 2013. Satellite synthetic aperture radar in archaeology and cultural landscape: an overview. Archaeol. Prospect. 20, 71–78. https://doi.org/10.1002/arp.1452.

Lightfoot, K.G., Cerrato, R.M., 1989. Regional patterns of clam harvesting along the atlantic coast of north America. Archaeol. E. N. Am. 17, 31–46.

Marquardt, W.H., 2010. Shell mounds in the southeast: middens, monuments, temple mounds, rings, or works? Am. Antiq. 75, 551–570. https://doi.org/10.7183/0002-7316.75.3.551.

Middaugh, D.P., 2013. Evidence of an archaic dam in a Carolina bay: the sewee shell ring, South Carolina. J. N. C. Acad. Sci. 129, 9–19.

Moore, C.B., 1894a. Certain sand mounds of the St. John's River, Florida, Part I. J. Acad. Nat. Sci. Phila. 10, 1–103.

Moore, C.B., 1894b. Certain sand mounds of the st. John's river, Florida, Part II. J. Acad. Nat. Sci. Phila. 10, 129–246.

Orengo, H.A., Conesa, F.C., Garcia-Molsosa, A., Lobo, A., Green, A.S., Madella, M., Petrie, C.A., 2020. Automated detection of archaeological mounds using machine-learning classification of multisensor and multitemporal satellite data. Proc. Natl. Acad. Sci. Unit. States Am. 202005583 https://doi.org/10.1073/pnas.2005583117.

Peacock, E., Rafferty, J., Hogue, S.H., 2005. Land snails, artifacts and faunal remains: understanding site formation processes at Prehistoric/Protohistoric sites in the Southeastern United States. In: Bar-Yosef, D. (Ed.), Archaeomalacology: Molluscs in Former Environments of Human Behavior. Oxbow Books, Oxford, pp. 6–17.

Putnam, F.W., 1875. List of items from mounds in New Madrid County, Missouri, and brief description of excavations. In: Harvard University, Peabody Museum, Eighth Annual Report, pp. 16–46.

Python Software Foundation, 2020. Python Language Reference.

R Core Team, 2020. R: A Language and Environment for Statistical Computing. R Foundation for Statistical Computing, Vienna, Austria.

Raymond, T.R., 2020. Testing for a functional relationship between shell rings and flood-prone environments in the yazoo basin of the lower Mississippi alluvial valley (M.A. Thesis). Mississippi State University.

Reitz, E.J., 1988. Evidence for coastal adaptations in Georgia and South Carolina. Archaeol. E. N. Am. 16, 137–158.

Ren, S., He, K., Girshick, R., Sun, J., 2017. Faster R-CNN: towards real-time object detection with region proposal networks. IEEE Trans. Pattern Anal. Mach. Intell. 39, 1137–1149. https://doi.org/10.1109/TPAMI.2016.2577031.

Russo, M., 2006. Archaic shell rings of the Southeast U.S.: national historic landmarks historic context. Southeast Archeological Center, National Park Service, Tallahassee.

Russo, M., 2004. Measuring shell rings for social inequality. In: Gibson, J.L., Carr, P.J. (Eds.), Signs of Power: the Rise of Cultural Complexity in the Southeast. University of Alabama Press, Tuscaloosa, pp. 26–70.

Sanger, M.C., 2017. Coils, slabs, and molds: examining community affiliation between Late Archaic shell ring communities using radiographic imagery of pottery. SE. Archaeol. 36, 95–109. https://doi.org/10.1080/0734578X.2016.1267466.

Sanger, M.C., Hill, M.A., Lattanzi, G.D., Padgett, B.D., Larsen, C.S., Culleton, B.J., Kennett, D.J., Dussubieux, L., Napolitano, M.F., Lacombe, S., Thomas, D.H., 2018. Early metal use and crematory practices in the American Southeast. Proc. Natl. Acad.

Sci. Unit. States Am. 115, E7672–E7679. https://doi.org/10.1073/pnas.1808819115.
Sanger, M.C., Ogden, Q.-M., 2018. Determining the use of Late Archaic shell rings using lithic data: "ceremonial villages" and the importance of stone. SE. Archaeol. 37, 232–252. https://doi.org/10.1080/0734578X.2017.1398995.
Sanger, M.C., Quitmyer, I.R., Colaninno, C.E., Cannarozzi, N., Ruhl, D.L., 2019. Multiple-proxy seasonality indicators: an integrative approach to assess shell midden formations from late archaic shell rings in the coastal Southeast north America. J. Isl. Coast. Archaeol. 1–31. https://doi.org/10.1080/15564894.2019.1614116.
Saunders, R., 2017. Archaic shell mounds in the American southeast. Oxford Handbooks Online. Oxford University Press. https://doi.org/10.1093/oxfordhb/9780199935413.013.75.
Somrak, M., Džeroski, S., Kokalj, Ž., 2020. Learning to classify structures in ALS-derived visualizations of ancient maya settlements with CNN. Rem. Sens. 12, 2215. https://doi.org/10.3390/rs12142215.
Soroush, Mehrtash, Khazraee, Ur, 2020. Deep learning in archaeological remote sensing: automated qanat detection in the kurdistan region of Iraq. Rem. Sens. 12, 500. https://doi.org/10.3390/rs12030500.
Squier, E.G., Davis, E.H., 1848. Ancient Monuments of the Mississippi Valley: Comprising the Results of Extensive Original Surveys and Explorations. Smithsonian Institution.
Swallow, G.C., 1858. Indian mounds in new madrid county, Missouri. Trans. Acad. Sci. St. Louis 1, 36.
Tan, C., Sun, F., Kong, T., Zhang, W., Yang, C., Liu, C., 2018. A survey on deep transfer learning. International Conference on Artificial Neural Networks. Springer, pp. 270–279.
Thompson, V.D., Andrus, C.F.T., 2011. Evaluating mobility, monumentality, and feasting at the Sapelo island shell ring complex. Am. Antiq. 76, 315–343. https://doi.org/10.7183/0002-7316.76.2.315.
Thompson, V.D., Turck, J.A., 2009. Adaptive cycles of coastal hunter-gatherers. Am. Antiq. 74, 255–278.
Trier, Ø.D., Cowley, D.C., Waldeland, A.U., 2019. Using deep neural networks on airborne laser scanning data: results from a case study of semi-automatic mapping of archaeological topography on Arran. Scotland. Archaeol. Prospect. 26, 165–175. https://doi.org/10.1002/arp.1731.
Trier, Ø.D., Reksten, J.H., Løseth, K., 2021. Automated mapping of cultural heritage in Norway from airborne lidar data using faster R-CNN. Int. J. Appl. Earth Obs. Geoinformation 95, 102241. https://doi.org/10.1016/j.jag.2020.102241.
Trinkley, M.B., 1985. The form and function of South Carolina's early woodland shell rings. In: Dickens, R.S., Ward, H.T. (Eds.), Structure and Process in Southeastern Archaeology. University of Alabama Press, Tuscaloosa, pp. 102–118.
Trinkley, M.B., 1980. Investigation of the Woodland Period along the South Carolina Coast (PhD Dissertation). University of North Carolina, Chapel Hill.
Verschoof-van der Vaart, W.B., Lambers, K., 2019. Learning to look at LiDAR: the use of R-CNN in the automated detection of archaeological objects in LiDAR data from The Netherlands. J. Comput. Anal. Appl. 2, 31–40. https://doi.org/10.5334/jcaa.32.
Willey, G.R., 1939. Ceramic stratigraphy in a Georgia village site. Am. Antiq. 5, 140–147.